Surface stress of partially H-covered Si(001) surfaces

Jan van Heys and Eckhard Pehlke*
Institut für Theoretische Physik und Astrophysik, Christian-Albrechts-Universität zu Kiel, D-24098 Kiel, Germany
(Received 28 April 2005; revised manuscript received 26 July 2005; published 30 September 2005)

Surface stress and chemisorption energy have been calculated for partially hydrogen-covered Si(001) surfaces by means of density-functional total-energy calculations. A stronger variation of the stress component $\sigma_\perp$ perpendicular to the Si-dimer bond with hydrogen coverage and adsorption geometry is observed as for the stress component $\sigma_\parallel$ parallel to the dimer bond. An approximation is suggested to generalize the *ab initio* results computed for periodically repeated (2×2) surface unit cells to arbitrary H-adsorption patterns on macroscopic surfaces. Surface stress as function of hydrogen coverage is presented for surfaces randomly covered with hydrogen atoms and for surfaces in thermodynamic equilibrium.

DOI: 10.1103/PhysRevB.72.125351 PACS number(s): 68.35.Gy, 68.43.Fg, 73.20.−r

I. INTRODUCTION

Besides step energies and other defect energies two important physical properties of the perfect surface enter into the continuum theory of solid surfaces and determine their morphology on mesoscopic length scales. These are the surface energy and the surface stress. The surface energy γ denotes the energy needed to create a certain patch of surface, whereas the surface stress σ describes the change of surface energy when the surface is strained.[1,2] Although, in the case of liquids, one does not have to distinguish between these two entities, they distinctly differ for solid surfaces. If surface symmetry is low, as is, for instance, the case for Si(001), then the surface energy variation depends on the direction of the applied strain, and hence the surface stress becomes anisotropic. Both surface energy and surface stress can be derived from total-energy calculations within the framework of density-functional theory.[3,4]

Various physical sources for surface stress are known to be active for different clean or adsorbate-covered surfaces.[1,5,6] Such are effects due to the surface electronic structure, strained bonds at the surface, which apply a stress to the bulk crystal, or atom-size effects, which are, in general, important for heteroepitaxial films.

A quantitative physical understanding of surface stress is essential. It not only lays the basis for various surface instabilities and the sometimes intriguing surface morphology observable on mesoscopic length scales, but because of the intimate link between surface stress and the electronic and geometric structure of the surfaces, its investigation can substantially add to our understanding of solid surfaces.

The technologically important Si(001) surface represents the drosophila of semiconductor surface physics. Its exciting properties, for example, the dimer buckling[7] or chemisorption dynamics,[8–10] have attracted researchers for a very long time. The surface stress parallel and perpendicular to the direction of the Si-dimer bond has been calculated for the clean surface by various groups.[11–16] In particular, it turned out that the alternating dimer buckling along the dimer rows on the $p(2\times2)$ or $c(4\times2)$ reconstructed Si(001) surface has to be carefully accounted for, as the stress differs significantly from that of a hypothetical (1×2) reconstructed surface with either buckled or symmetric dimers.[13,16] Part of this difference is due to the additional relaxation of the second layer silicon atoms, which is possible only in the case of the larger surface unit cell of the Si(001)-$p(2\times2)$ or $c(4\times2)$ reconstructions.

A chemisorbed hydrogen atom selectively saturates the dangling bond of the individual Si surface-atom to which it is attached and thereby strongly perturbes the electronic structure of the surface. If a single dangling bond of a Si-dimer is saturated by a hydrogen atom, the remaining dangling bond lacks its charge-transfer partner in order to decrease its energy according to the well-known Jahn-Teller-like mechanism active on the clean surface. In some cases, however, a Jahn-Teller (JT) coupling between dangling bonds on adjacent Si-dimers can be observed instead, as will be demonstrated below. The strong perturbation of the electronic structure of the Si(001) surface due to single adsorbed H atoms results in a dramatical increase of surface reactivity, as has previously been demonstrated, both experimentally and theoretically.[9,17,18]

In this paper, we focus on the change of surface stress when dangling bonds on the Si(001) surface become successively saturated with H atoms. All different chemisorption configurations that are possible within a periodically repeated (2×2) surface unit cell have been considered. As H atoms tend to pair on Si surface-dimers,[19] most of these configurations are only metastable. However, such configurations can be prepared, experimentally, simply by adsorbing hydrogen atoms at a temperature for which H-atom diffusion is sufficiently slow.[17] As a possible application of the present theoretical results, we suggest that the equilibration dynamics of such metastable configurations due to the diffusion of the hydrogen atoms on the surface might be experimentally observable within some temperature range by monitoring the time-dependent variation of an appropriate surface stress component on, e.g., a single-domain vicinal Si(001) surface.

II. COMPUTATIONAL METHOD

The ground-state energies and relaxed geometries of partially H-covered Si(001) surfaces have been computed using the total-energy package FHI96MD[20] from the Fritz-Haber In-

stitute in Berlin. The calculations are based on density-functional theory, with the generalized gradient approximation by Perdew *et al.*[21] (PBE-GGA) being applied to the exchange-correlation energy functional. A Hamann pseudopotential has been generated for the silicon atom by means of the code FHI98PP,[22] in which, for the sake of consistency, the same PBE-GGA has been applied to the exchange-correlation energy functional. For the hydrogen atom, the full $1/r$ Coulomb-potential has been used. The H-atom potential requires a kinetic-energy cutoff of the plane-wave basis set of 40 Ry, whereas 16 Ry is sufficient for calculations including only Si atoms. Convergence tests have been carried out with cutoff energies up to 60 Ry for systems containing H atoms, and the error is estimated to be <0.5 meV/Å^2 in case of the stress anisotropy. This result was derived for the monohydride configuration. The various adsorption configurations have been simulated with 12 or 16 atomic layer thick Si slabs and supercells with a (1×2) or (2×2) surface unit cell. We use symmetric slabs with the same surface reconstruction and adsorption configuration on both sides of the slab. All possible configurations for H atoms adsorbed within a (2×2) surface unit cell have been considered. The H coverages thus amount to $\Theta=0$, 1/4, 1/2, 3/4, and 1 (Fig. 1). The slabs, which are periodically repeated in the direction perpendicular to the surface, are separated by a vacuum region with a thickness equivalent to at least six Si-bulk layers. Different vacuum thicknesses have been tested, and the above value has been shown to be sufficient. The integrals over the Brillouin zone are approximated by sums over special **k**-points,[23] using **k**-point meshes with 36 **k**-points within the first Brillouin zone of the $p(2\times2)$ reconstructed surface. Additional convergence tests have been carried out with up to 64 **k**-points in the full first Brillouin zone for semiconducting surfaces and with up to 200 **k**-points for metallic surfaces.

As a rule, basis set corrections[24] ought to be considered when the size of the supercell is varied, e.g., when the lattice constant is altered or the slab is strained. This correction has been accounted for where necessary, however, because of the large basis-set cutoff energy, it is negligible in most of the calculations described below. The equilibrium lattice constant of Si was calculated to be $c=5.47$ Å, reproducing the slight overestimate of the experimental lattice constant of 5.43 Å known for various GGAs in case of silicon.[25] Si slabs with the theoretical lattice constant have been relaxed until the residual forces are less than 2×10^{-4} H/bohr. No inner layers were artificially kept fixed. This ensures that there are no residual forces acting on the inner layers, which elsewise could spoil the stress calculation.

The surface stress tensor[1] σ_{ij} is defined by

$$\Delta E_{\mathrm{surf}} = A\sum_{i,j=1}^{2}\sigma_{ij}\varepsilon_{ij}. \tag{1}$$

It describes, to linear order in the strain, the change of surface energy $E_{\mathrm{surf}}=\gamma A$ of a patch of surface of area A in response to an applied strain ε_{ij}. In the case of the Si(001) surface, the surface stress tensor becomes diagonal in a coordinate system with axes pointing in the [110] and [$\bar{1}$10] directions. The respective stress components parallel or perpendicular to the Si-dimer bond are denoted by $\sigma_{\parallel}$ and $\sigma_{\perp}$, respectively.

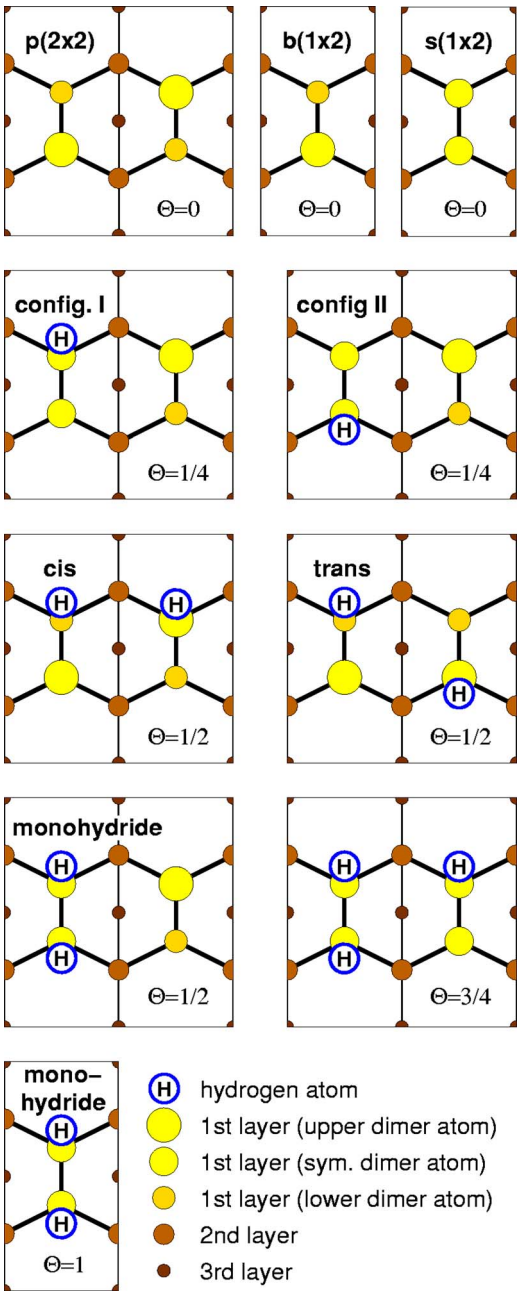

FIG. 1. (Color online) Schematic representation of surface unit cells and adsorption geometries for H-coverages $\Theta=0$, 1/4, 1/2, 3/4, and 1 within a (2×2) surface cell.

We compute $\sigma_{\parallel}$ and $\sigma_{\perp}$ almost directly from this definition. To this purpose we strain the slab either parallel to the [110] or parallel to the [$\bar{1}$10] direction, with the absolute value of the strain $|\varepsilon_{ii}|\leqslant0.04$. Perpendicular to the surface the slab is strained according to a computed strain ratio $\tilde{\nu}=0.367$ (corresponding to mechanical equilibrium in the direction perpendicular to the surface, i.e., $\tilde{\nu}$ is conceptually similar, but not identical to, the Poisson ratio ν).[26] $\tilde{\nu}$ compares well to the respective value of $c_{12}/c_{11}=0.39$[27] from

classical elasticity theory. An additional relaxation of the atomic positions within the supercell is not necessary as long as only the stress at the equilibrium bulk Si lattice constant is to be calculated, because the energy gain due to such a relaxation constitutes a contribution of second and higher order in the strain, whereas the stress, on the other hand, gives an account of the first-order variation of the total energy with applied strain.

It is impractical to derive the surface stress components directly from the total energy E_{tot} as a function of applied strain because E_{tot} is dominated by large contributions from the bulk elastic energy. This problem can be lifted, however, by computing total energies, $E_{\mathrm{total}}^{(12)}$ and $E_{\mathrm{total}}^{(16)}$, for two slabs, which are 12 and 16 layers thick, because all bulk contributions can be subtracted out via

$$E_{\mathrm{surf}}(\varepsilon_{\parallel},\varepsilon_{\perp}) = 4E_{\mathrm{tot}}^{(12)}(\varepsilon_{\parallel},\varepsilon_{\perp}) - 3E_{\mathrm{tot}}^{(16)}(\varepsilon_{\parallel},\varepsilon_{\perp}). \tag{2}$$

The surface stress components $\sigma_{\parallel}$ and $\sigma_{\perp}$ are easily derived from the slope of $E_{\mathrm{surf}}(\varepsilon_{\parallel},\varepsilon_{\perp})$ at the equilibrium Si lattice constant, i.e., for $\varepsilon_{\parallel}=\varepsilon_{\perp}=0$. For example, we obtain $\sigma_{\parallel}$ from

$$E_{\mathrm{surf}}(\varepsilon_{\parallel},0) = E_{\mathrm{surf}}(0,0) + 2A\sigma_{\parallel}\varepsilon_{\parallel} + \mathcal{O}(\varepsilon_{\parallel}^2). \tag{3}$$

The factor of two in the prefactor $2A$ has been inserted in order to explicitly account for the top and bottom surface of the slab.

On the other hand, the stress anisotropy,

$$\Delta\sigma = \sigma_{\parallel} - \sigma_{\perp}, \tag{4}$$

can be derived from total energies as a function of strain for a single-layer thickness alone, because the bulk contributions cancel automatically due to the symmetry of the bulk crystal

$$E_{\mathrm{total}}^{(16)}(\varepsilon,0) - E_{\mathrm{total}}^{(16)}(0,\varepsilon) = 2A\varepsilon\Delta\sigma + \mathcal{O}(\varepsilon^2). \tag{5}$$

Apart from the stress calculation using total energy differences as described above, we have carried out additional *ab initio* stress calculations using the code ABINIT by Gonze *et al.*,[28] which makes use of an analytical stress tensor.[29] In these calculations, the stress components parallel to the surface have been corrected in the usual way by subtracting σ_{zz} (Pulay stress[24,30]), the residual stress component in the direction perpendicular to the surface. We found a very satisfying agreement between the two methods, as will be detailed in the Appendix.

III. RESULTS AND DISCUSSION

A. Clean surface

As a reference system, and in order to compare to previously published theoretical work, we have carried out stress calculations for reconstructions of the clean Si(001) surface with symmetric or buckled dimers. Some of these reconstructions are only hypothetical, i.e., they have been used before for theoretical considerations, but they do not appear as ground-state structures on the real surface.

With $s(1\times2)$ we denote a surface reconstruction with Si surface-dimers where the dimer bond is artificially kept parallel to the surface plane. $b(1\times2)$ denotes a (1×2) reconstruction with a buckled dimer, and $p(2\times2)$ a reconstruction with a (2×2) surface unit cell where the buckling angle alternates along the dimer rows. The latter one is similar to the $c(2\times4)$ reconstruction, which differs from the $p(2\times2)$ reconstruction only in an additional shift of the dimer buckling pattern by one lattice constant parallel to the dimer rows every second row. Surface energies[31] and stresses (Table II) are similar for these two reconstructions. When comparing to experimental results measured at some finite temperature one has to account for thermally excited dimer flips, which create local $b(1\times2)$ buckled configurations that can propagate over the surface. At high temperatures, dimer flips independent of the buckling angle of the neighboring Si dimers are often

TABLE I. Surface stress of the clean Si(001) surface calculated within the LDA for exchange and correlation in comparison to data from the literature.

Source and method	Surface reconstruction	$\sigma_{\parallel}$	$\sigma_{\perp}$ (meV/Å^2)	$\Delta\sigma$
Webb *et al.*,[35] exp.	clean			60–80
Alerhand *et al.*,[15] Tight-binding	$s(1\times2)$	36	−80	116
	$b(1\times2)$	35	−35	70
Payne *et al.*,[14] DFT-LDA	$s(1\times2)$	47	−132	179
Meade and Vanderbilt,[12] DFT-LDA	$s(1\times2)$	106	−60	166
Liu and Lagally,[11] DFT-LDA	$s(1\times2)$	73	−129	202
Liu and Lagally,[11] Tersoff Potential	$s(1\times2)$	32	−78	110
García and Northrup,[13] DFT-LDA	$s(1\times2)$	130	−27	164
	$b(1\times2)$	144	21	123
	$c(4\times2)$	157	102	55
Dąbrowski *et al.*,[16] DFT-LDA	$s(1\times2)$	$\sigma_{\parallel}^{s}$	$\sigma_{\perp}^{s}$	150
	$b(1\times2)$	$\sigma_{\parallel}^{s}+30$	$\sigma_{\perp}^{s}+75$	105
	$p(2\times2)$	$\sigma_{\parallel}^{s}+30$	$\sigma_{\perp}^{s}+125$	55
This work, DFT-LDA	$p(2\times2)$	65	20	47

TABLE II. Surface stress of several reconstructions of the clean Si(001) surface. All values have been computed with the PBE-GGA applied to the exchange-correlation energy-functional. Note that the data for the metallic $s(1\times2)$ reconstruction (which, for reasons of symmetry, has been calculated using thinner slabs with only 10 and 14 Si layers) are less accurate than the data for the semiconducting surface structures.

Surface reconstruction	$\sigma_{\parallel}$	$\sigma_{\perp}$ (meV/Å^2)	$\Delta\sigma$
$s(1\times2)$	36	−91	108
$b(1\times2)$	84	−12	97
$p(2\times2)$	77	38	39
$c(4\times2)$[47]	78	38	40

assumed. The effect on the stress has already been estimated by Dąbrowski *et al.*,[32] for this reason we do not go into any further detail here.

In the present work the emphasis is on systems containing hydrogen-silicon bonds; therefore, we consistently apply the PBE-GGA instead of the local-density approximation (LDA) to the exchange-correlation energy-functional. To be able to compare to previous LDA work, however, we have carried out a few additional calculations using LDA instead of PBE-GGA. We remark that, although the GGA, e.g., improves upon the reaction barriers of hydrogen with silicon[33] and is therefore used by default for such systems, it is not clear whether GGA or LDA will yield the more reliable surface stress for the clean surface. As can be read from Tables I and II, in the case of the $p(2\times2)$ reconstructed clean Si(001) surface, the differences between LDA and PBE stresses are 12, 18, and 8 meV/Å^2 for $\sigma_{\parallel}$, $\sigma_{\perp}$, and $\Delta\sigma$, respectively.

The $p(2\times2)$ reconstructed Si(001) surface is characterized by buckled dimers with a dimer bond length of 2.36 Å (calculation with PBE and 16 Si layers) and a buckling angle of ±19°, which alternates along each dimer row. The Si atoms in the second layer relax by ±0.1 Å parallel to the dimer row. The Si atom, which relaxes inward, pushes its second nearest neighbors aside. The electronic structure is governed by the rehybridization of the Si sp^3 hybrid orbitals and the formation of an occupied dangling bond orbital at the Si atom that has relaxed outward, and a predominantly p-like unoccupied dangling bond orbital at the Si atom that has relaxed inward. The dimer buckling[34] can, thus, be ascribed to a Jahn-Teller-like mechanism. The surface energy, derived from the total energy difference between a 16 and 12-layer thick slab, is plotted in Fig. 2 as a function of strain. Apart from the prefactor $2A$, the surface stress is equal to the slope at $\varepsilon=0$, i.e., $\sigma_{\parallel}=77$ meV/Å^2 and $\sigma_{\perp}=38$ meV/Å^2. These two stress components are consistent with the stress anisotropy $\Delta\sigma=39$ meV/Å^2 derived solely from the 16-layer thick slab. As demonstrated in Fig. 3, an additional relaxation of the atom positions within the supercell does not affect the result. The tensile stress parallel to the dimer bond is attributed to the top-layer Si-dimerization: Pairs of Si atoms, which would be next-nearest neighbors in the bulk, are tilted toward each other to form the dimer bond. When the lattice constant is reduced, while the dimer bond length stays

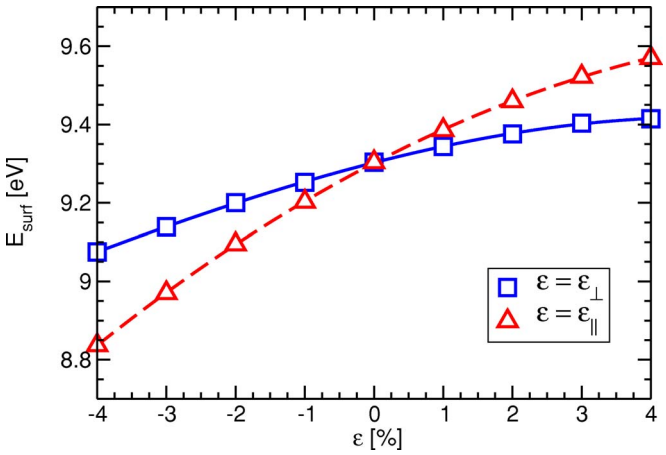

FIG. 2. (Color online) Energy $E_{\mathrm{surf}}=2\gamma A$ of the clean $p(2\times2)$ reconstructed Si(001) surface as a function of strain ε, with A equal to the area of the (2×2) surface unit cell. Blue squares: slab strained perpendicular to the dimer bond. Red triangle: slab strained parallel to the dimer bond. Note that the slabs have not been atomically relaxed again after straining. The surface stress components $\sigma_{\perp}$ and $\sigma_{\parallel}$ have been derived from the slope of these curves at $\varepsilon=0$.

the same, the atoms move into a more bulklike configuration with respect to bond angles. This configuration is energetically preferable. Thus, the Si-dimers exert a tensile stress on the Si bulk parallel to the dimer bond. Perpendicular to the dimer bond, the stress comes out tensile for this reconstruction.

On the $b(1\times2)$ reconstructed surface all dimers buckle in the same direction. The buckling angle becomes only slightly smaller, $\theta=17.5°$, and the dimer bond length equals 2.31 Å. Because of the small surface unit cell, no relaxation of the second-layer atoms parallel to the dimer rows is possible any

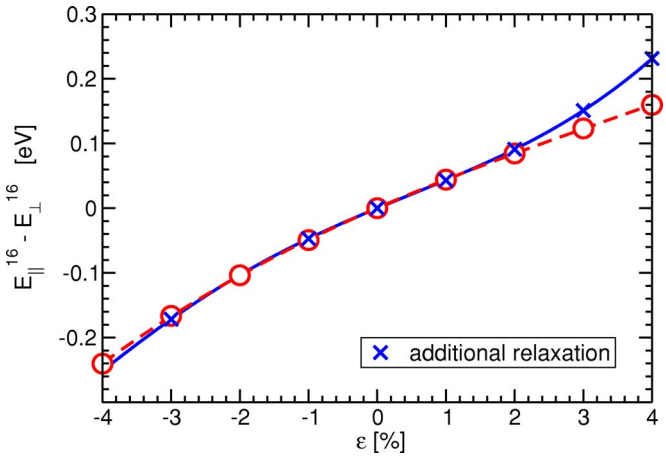

FIG. 3. (Color online) Energy difference $E_{\mathrm{surf}}(\varepsilon,0)-E_{\mathrm{surf}}(0,\varepsilon)$ for the clean $p(2\times2)$ reconstructed Si(001) surface as a function of strain ε. The surface area amounts to two (2×2) surface unit cells. Results are for a 16-layer thick slab. The stress anisotropy $\Delta\sigma$ is derived from the slope at $\varepsilon=0$. Red line and circles: slab strained as explained in the text, no additional relaxation. Blue line and crosses: data after additional relaxation of all atom positions in the supercell.

TABLE III. Surface stress of hydrogen covered Si(001) surfaces for all hydrogen coverages Θ and adsorption geometries compatible with a periodically repeated $p(2\times2)$ surface unit-cell. ΔE denotes the energy difference per 2×2 surface unit-cell with respect to the average energy of a macroscopic surface where all hydrogen atoms are condensed into a large monohydride ($\Theta=1$) island, while the rest of the surface is clean. (This fully facetted configuration corresponds to the zero-temperature ground-state of the surface.) The adsorption geometries are described in the text. If not stated otherwise, all calculations are for spin-unpolarized surfaces.

Surface coverage	$\sigma_{\parallel}$	$\sigma_{\perp}$ (meV/Å^2)	$\Delta\sigma$	ΔE meV/$p(2\times2)$
$\Theta=0$, clean	77	38	39	Ref.
$\Theta=1$, monohydride	72	2	70	Ref.
$\Theta=1/2$, monohydride	70	−4	78	58
$\Theta=1/2$, *cis*	60	29	31	255
$\Theta=1/2$, *trans*	58	22	39	459
$\Theta=1/4$, config. I	60	1	57	274
$\Theta=1/4$, config. II	59	−50	107	285
$\Theta=3/4$	66	−2	73	314
$\Theta=3/4$, spin polarized	68	1	72	176

more. The electronic structure closely resembles the electronic structure of the $p(2\times2)$ reconstruction. While the surface stress parallel to the dimer bond is nearly the same within the error bars as for the $p(2\times2)$ reconstruction, the stress $\sigma_{\perp}=-12$ meV/Å^2 perpendicular to the dimer bond becomes compressive.

The $s(1\times2)$ reconstruction with symmetric dimers (with the dimer bond length equal to 2.31 Å) differs in several respects from above reconstructions with buckled dimers. It is not metastable, but its particular geometry has to be enforced by employing an artificial mirror plane perpendicular to the dimer bond. Moreover, the surface band structure is metallic, what renders the structure energetically unfavorable.[34] The surface bands are derived from dangling bond states of the Si-dimer forming π-bonding and π-antibonding combinations. While the stress parallel to the dimer bond is tensile, the stress perpendicular to the dimer bond becomes strongly compressive, $\sigma_{\perp}=-91$ meV/Å^2. This may partially be due to a preference of the Si surface atoms for a more planar bond configuration, owing to an energy gain by sp^2+p rehybridization.

Stress data published before by various groups have been collected in Table I. Note that the experimental value by Webb *et al.*[35] constitutes a thermal stress average and thus should not be compared to any theoretical result for one single reconstruction alone.[16] The comparison to our results is hampered by the large span of the data. Although our two stress components are less tensile than those by Garcia and Northrup,[13] there is a reasonable overall consensus with respect to the stress differences between different reconstructions. Our final PBE results are summarized in Table II.

B. Partially H-covered Si(001) surfaces

It is well known that in thermodynamic equilibrium the H atoms (or, what yields the same consequences, the dangling bonds) tend to pair on the Si dimers.[19,38] Moreover, the H-covered dimers tend to cluster, but the respective interdimer interaction energy is much smaller than the energy gained by pairing.[36,37] At finite temperature, due to entropic reasons, clean dimers and dimers with one or both dangling bonds saturated by H atoms will intermix. Moreover, such configurations can be prepared in excess of their equilibrium density by adsorbing atomic hydrogen at sufficiently low temperatures where H diffusion on the surface is frozen in.[17] To investigate the surface stress of such partially H-covered surfaces, we have calculated stress and energy for all H-adsorption configurations that are compatible with a periodically repeated $p(2\times2)$ surface unit cell. The relaxed atomic and electronic structure of the equilibrium surface reconstructions are described, in detail, below; and the results for the surface stress components are summarized in Table III. As an energy reference we always take the macroscopic zero-temperature ground-state situation, i.e., a surface that consists of two large patches, one displaying the clean $p(2\times2)$ reconstructed surface, and the other one being fully H saturated (monohydride configuration). The estimated accuracy of the calculated data is about ±7 meV/Å^2 for the stress tensor components and ±4 meV/Å^2 for the stress anisotropy. This error estimate accounts for the small uncertainties due to the fit through the calculated data points; moreover, it includes results from convergence tests with respect to the thickness of the slab (from a comparison between 12 and 16 layers), the thickness of the vacuum region, the cutoff energy of the plane-wave basis set, and the number of **k**-points used for the approximation of the integrals over the Brillouin zone. Variations due to the approximation applied to the exchange-correlation energy functional are not covered by this error bar.

1. Full coverage, $\Theta=1$

At full H coverage, $\Theta=1$, a monohydride surface forms on which all Si dangling bonds are saturated with hydrogen

atoms. In this case still all Si surface dimers stay intact. Only at even higher H coverages, which, however, are not addressed in this paper, the Si-Si dimer bonds break and dihydride groups form on the surface. Because of the saturation with H atoms, the dangling-bond derived surface-state bands vanish from the principle gap of the surface band structure, and thus there is no electronic driving force toward dimer buckling any more. Consequently, the Si dimer of the monohydride group is parallel to the surface. Presumably because of the lack of the additional π bond, the Si-Si dimer bond length of 2.41 Å comes out somewhat larger than for the clean symmetric dimer (2.31 Å).

The tensile stress parallel to the Si dimer bond $\sigma_{\parallel}=72$ meV/Å^2 is almost the same as for the clean buckled dimers in the $p(2\times2)$ configuration (77 meV/Å^2), whereas, in the direction perpendicular to the dimer bond, the stress is significantly reduced from 38 meV/Å^2 for the clean $p(2\times2)$ reconstructed surface to $\sigma_{\perp}=2$ meV/Å^2 for the monohydride surface. This may be interpreted in the following way: The tensile stress parallel to the dimer bond is a consequence of the strained Si-bond configuration on the surface, which stays intact after hydrogen adsorption. The compressive stress of the clean Si(001)-$s(1\times2)$ surface (with symmetric dimers) perpendicular to the dimer bond may be ascribed to a tendency of the Si atoms carrying a half-filled dangling bond to acquire a more planar bond configuration. The almost vanishing perpendicular stress component on the monohydride surface would then be consistent with the notion that this electronic-structure-driven stress effect vanishes when the dangling bond states become saturated by H atoms.

2. Half coverage, $\Theta=1/2$

Among all periodically repeated (2×2) surface unit cells containing two adsorbed H atoms, the configuration with one monohydride dimer next to a clean Si dimer yields the smallest surface energy, which is only 58 meV per (2×2) surface unit cell larger than our reference energy referring to H islanding [i.e., half of the macroscopic Si(001) surface is assumed to be H covered in the monohydride configuration, $\Theta=1$, whereas the other half is perfectly clean, $\Theta=0$]. This result is in agreement with the clustering interaction energy for hydrogen atoms adsorbed on the terraces of vicinal Si(001) surfaces previously calculated.[37] In accordance with this small interaction energy, the structure of the two Si dimers is similar to what we have found for the monohydride group on the one hand, and the clean Si-dimer on the $b(1\times2)$ surface on the other hand. The Si—Si bond of the H—Si—Si—H group is tilted by only −0.8° with respect to the surface plane, whereas the buckling angle of the clean Si-dimer is equal to 17.6°, which is virtually the same as the 17.5° calculated for the $b(1\times2)$ reconstruction. The same similarity also holds true for the Si dimer bond lengths, which equal 2.41 and 2.32 Å for the H-covered and the clean dimer, respectively. The surface electronic structure is semiconducting. It is governed by the typical occupied and unoccupied rehybridized dangling-bond states, which derive from the two inequivalent Si atoms of the clean buckled dimer.

The surface stress parallel to the dimer bond has been calculated to be 70 meV/Å^2 parallel to the dimer bond and marginally compressive, −4 meV/Å^2, perpendicular to the dimer bond. The latter result is roughly compatible with an average of the stress perpendicular to the dimer bond of the monohydride surface and the clean $b(1\times2)$ dimerized surface with buckled dimers. For the stress parallel to the dimer bond, the same simple averaging would yield 78 meV/Å^2, which is larger than the exact result by 8 meV/Å^2.

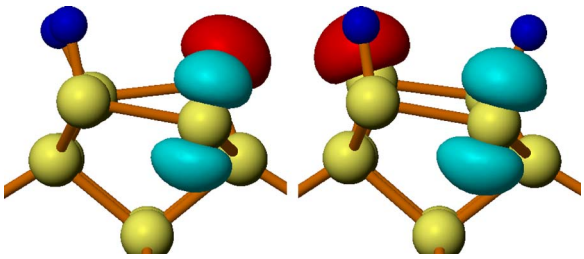

FIG. 4. (Color online) Sideview of the atomic geometry in the *cis*- (left) and in the *trans*-configuration (right). Contour surfaces of constant electron density are displayed for (i) the occupied dangling bond orbital (red) at the outward-relaxed Si-dimer atom and (ii) the *p*-like empty dangling bond orbital (light blue) at the inward-relaxed Si-dimer atom. In case of the cis-configuration the Jahn-Teller-like mechanism requires an alternating buckling angle, whereas in case of the *trans*-configuration, both dimers buckle in the same direction.

The total energy of the adsorbate structure increases distinctly when the two hydrogen atoms are not attached to the same but to the two different Si dimers in the $p(2\times2)$ unit cell. Two different configurations have to be distinguished: In the *cis*-configuration, the H atoms occupy neighboring sites located at the same end of the two Si dimers, whereas in the *trans*-configuration the H atoms are attached to the Si atoms at opposite sides of the two dimers. In case of the *cis*-configuration, the energy increases by 255 meV per (2×2) surface unit cell, and in case of the *trans*-configuration by even more, 459 meV/(2×2) surface unit cell,[39] both energies being measured with respect to the reference surface.

In the *cis*-configuration, the buckling angles of the two dimers are of opposite sign (i.e., the buckling angle alternates as in the $p(2\times2)$ reconstruction), 10.3° and −6.5° (see Fig. 4). The dimer bond lengths amount to 2.39 and 2.45 Å, respectively. The electronic structure is again determined by rehybridization of the dangling bond orbitals and a Jahn-Teller-like effect. In this case, however, the JT coupling occurs between the dangling bond orbitals of the neighboring dimers. The calculated surface stress components are $\sigma_{\parallel}=60$ meV/Å^2, which might point toward a slightly weakened Si dimer bond, and $\sigma_{\perp}=29$ meV/Å^2.

Care has to be taken when computing the atomic geometry of the *trans*-configuration. Again, the total energy is minimized by a JT-like mechanism involving the two remaining unsaturated dangling bond states in the surface unit cell. However, as these orbitals are located at the two opposite sides of the Si dimers, to obtain the advantageous rehybridization of the orbitals in this case, the two dimers have to buckle in the same direction. The relaxed buckling angles amount to 7.4° and 10.0°, and the dimer bond lengths are 2.43 and 2.40 Å, respectively (see also Fig. 4). The calcu-

lated surface stress components are $\sigma_{\parallel}=58$ meV/Å^2 and $\sigma_{\perp}=22$ meV/Å^2.

3. Coverage $\Theta=1/4$

There arise two inequivalent adsorption geometries when a single hydrogen atom adsorbs within a $p(2\times2)$ surface unit cell. These geometries primarily differ by the direction of the buckling of the clean Si dimer: The Si atom of the clean dimer, which is on the same side as the H atom of the Si-H group, can either relax outward toward the vacuum region (configuration I) or inward (configuration II). In both cases, the clean Si-dimer buckles by 18°, while the buckling angle of the half H-saturated Si dimer is rather small, equal to −2° or −5° in case of configuration I and II, respectively. Also the energies of the two configurations of 274 and 285 meV per (2×2) surface unit cell have to be considered identical within the accuracy of the present calculation. In both cases the electronic structure is characterized by two Jahn-Teller-split either fully occupied or unoccupied dangling-bond states located on the clean buckled dimer (similar to the surface electronic structure of the clean surface) and a metallic state at the Fermi level predominantly derived from the remaining dangling bond orbital at the half H-saturated Si dimer.

Although the surface stress parallel to the dimer bond $\sigma_{\parallel}=60$ meV/Å^2 and 59 meV/Å^2 is also very similar for both configurations, the stress perpendicular to the dimer bond differs dramatically: It vanishes for configuration I, $\sigma_{\perp}=1$ meV/Å^2, but it becomes strongly compressive, $\sigma_{\perp}=-50$ meV/Å^2, for configuration II. This is in distinct contrast to the close similarity between the dimer buckling angles of the relaxed geometries.

4. Coverage $\Theta=3/4$

Within the (2×2) surface unit cell the atomic geometry at coverage 3/4 comes out uniquely. There remains a single Si dangling bond per surface unit cell, which is not H saturated and which is surrounded by monohydride groups. Energy and stress of the spin-unpolarized surface are given in Table III.

Additional calculations for this configuration with the code FHI96SPIN by Bockstedte,[40] however, showed that a spin-polarized electronic ground state is energetically preferable. Hence, the stress also had to be computed for the spin-polarized configuration, with the results summarized in Table III. As expected, the buckling angles are small, 0.1° for the monohydride dimer and 1.1° for the dimer carrying the single dangling-bond state. The dimer lengths are 2.41 and 2.40 Å. The surface energy amounts to 176 meV with respect to the reference state (cf. Table III). The stress equals 68 meV/Å^2 parallel to the dimer bond and practically vanishes (1 meV/Å^2) in the direction perpendicular to the dimer bond. These values are compatible with the stress data for the other configurations. Comparison of the spin-polarized with the spin-unpolarized calculation shows that the components of the stress tensor come out basically equal within the error bars, while the surface energy is lowered by about 138 meV/(2×2).

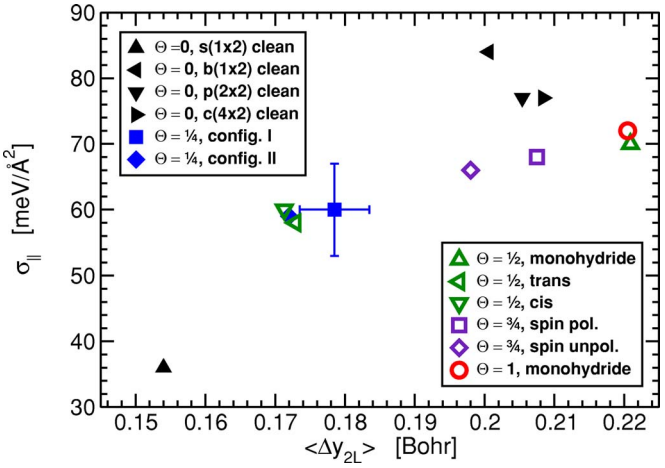

FIG. 5. (Color online) Correlation between the stress component $\sigma_{\parallel}$ and the average displacement of the second layer atoms Δy_{2L} from their bulk position. The error bar is representative for all data points, with the exception of the metallic $s(1\times2)$ surface.

5. Discussion of stress results

As can be read from Table III, the surface stress parallel to the dimer bond stays always tensile and varies only moderately in the range between 58 meV/Å^2, for H-coverage $\Theta=1/2$ (*trans*-config.), and 77 meV/Å^2 for the clean surface. Note, however, that the stress is not a monotonous function of hydrogen coverage. Physical reason for this tensile stress is the surface-dimer bond that stays intact for all configurations studied in this paper. For geometrical reasons—the dimer atoms are not nearest neighbors in the bulk diamond lattice—the dimer tends to contract the underlying crystal. This microscopic stress is mediated from the top layer to the second layer via the bond angle dependence of the interatomic potential. This simple mechanical picture is corroborated by Fig. 5, which shows a positive correlation between the relaxation Δy_{2L} of the second layer Si-atoms in the direction parallel to the dimer bond and $\sigma_{\parallel}$. A similar correlation with $\sigma_{\parallel}$ can also be observed in deeper layers for atomic displacements in particular directions determined by the mechanical coupling between the atoms in the diamond lattice.

The stress $\sigma_{\perp}$ in the direction perpendicular to the dimer bond varies over the range from −50 to 38 meV/Å^2. This range of variation is distinctly larger than in the case of $\sigma_{\parallel}$, even if we further restrict ourselves to low-energy configurations appearing on thermodynamically equilibrated surfaces. As becomes particularly striking when comparing the two configurations corresponding to $\Theta=1/4$, the stress depends sensitively on the particular surface geometry, it is not a function of the H coverage alone. This is consistent with the known sensitivity of stress on surface reconstruction details, e.g., in case of the clean surface (cf. Table II).

C. Random H distribution versus equilibrated surfaces

For future comparison to experiment we have to generalize above *ab initio* data to macroscopic Si(001) surfaces that are covered with some arbitrary adsorption patterns of hydrogen atoms. To estimate surface energy and surface stress

TABLE IV. Comparison of *ab initio* stress data with the simple estimate described in the text. In the case of a (3×2) unit cell, stresses for three different (2×2) cells are averaged over.

Surface reconstruction		$\sigma_{\parallel}$	$\sigma_{\perp}$ (meV/Å^2)	$\Delta\sigma$
$\Theta=1/2$, config. *A*	*ab initio*	65	−18	81
	average	66	−18	86
$\Theta=2/3$, config. *B*	*ab initio*[47]	69	16	53
	average	65	8	61

of such a random H-adsorption pattern, we cover the surface by overlapping (2×2) unit cells, which are displaced by one (1×1) surface lattice constant along the dimer row with respect to each other. An estimate for the average surface energy and surface stress of the macroscopic surface is derived by averaging over the respective contributions from all of these (2×2) cells.

This rather crude approach obviously neglects many adsorption-configuration-dependent details of the elastic and electronic interactions beyond the small (2×2) unit cells. To test it, we have computed the surface stress for two additional configurations with surface unit cells that are three dimers wide. Configuration *A* consists of a (2×2) cell with one hydrogen atom in configuration II next to a monohydride group. The hydrogen coverage is equal to $\Theta=1/2$. Configuration *B* consists of a (2×2) cell with two hydrogen atoms in a local *trans*-configuration next to a monohydride group. Accordingly, the hydrogen coverage is equal to $\Theta=2/3$. In Table IV the *ab initio* results are compared to the respective estimates derived from our averaging procedure described above. For configurations *A* and *B* the *ab initio* stress results are in semiquantitative agreement with the simple estimate from averaging, with an error $\leqslant 8$ meV/Å^2. However, there are configurations for which the difference will be larger. Consider, for example, a (2×3) surface unit cell with three adsorbed H atoms, one H atom per Si dimer, and the H atoms adsorbed at opposite sides of the dimer (*trans*-configuration). Preliminary test calculations yielded an error twice as large as above. In this case, however, the probable source of error is not the averaging scheme, but the choice of a too small unit cell in the *ab inito* calculations: There are three dangling-bond orbitals in the (2×3) cell, thus one dangling bond lacks a partner for energy relaxation by rehybridization and JT coupling. If the calculation were repeated with a (2×6) surface unit cell, which is, however, beyond the scope of this paper, then every dangling bond would have a partner for efficient energy relaxation by JT coupling and we speculate that the error between the *ab initio* stress for the (2×6) surface unit cell and our result from averaging ought to decrease. Certainly, much more work is needed to make the extrapolation from small-unit-cell atomic data to macroscopic surfaces more accurate.

Two extreme models have been considered for the mechanism of H-atom absorption. The first model is adequate for temperatures at which surface hydrogen diffusion can be neglected over the time span of the stress measurement. In that case, hydrogen atoms randomly impinge on the Si(001) surface and stick to the Si-dimer atom, where the H atom has hit the surface. If the site is already occupied, then the hydrogen atom is assumed to be reflected (i.e., any Eley-Rideal reaction is neglected).[41] A surface area of 2048 dimers has been simulated, and the result is shown in Fig. 6 as the blue curves.

When the surface is annealed, the hydrogen atoms start to diffuse over the surface. Thermodynamically equilibrated configurations have been generated, using the Metropolis Monte Carlo algorithm[45] together with a surface energy estimated by the averaging procedure described above. Results for temperature $T=450$ K are shown as red lines in Fig. 6. This temperature has been chosen close to the temperature where hydrogen diffusion on the Si(001) surface is supposed to become relevant.[17] The stress component $\sigma_{\parallel}$ becomes more tensile after equilibration at low coverages due to the vanishing of local high-energy surface configurations with solitary hydrogen atoms and compressive stress.

It should be noted that in both situations considered above the thermally excited dimer flip motion has been accounted for by calculating appropriate thermal averages (which are based on the calculated *ab inito* energies summarized in Table III) of the stresses. In the case of the clean surface, an average over the stresses for the $b(1\times2)$ and the $p(2\times2)$ reconstructions was used, and in case of $\Theta=1/4$ the stresses for configurations I and II were thermally averaged.

IV. SUMMARY AND CONCLUSIONS

By means of density-functional total-energy calculations for periodically repeated supercells with a (2×2) surface unit cell, surface energy and surface stress tensor have been computed for all possible configurations of hydrogen atoms adsorbed on a Si(001) $p(2\times2)$ surface unit cell. Hydrogen coverages range from 0 to 1. We observe a stronger variation of the stress component $\sigma_{\perp}$ with coverage and adsorption geometry than for $\sigma_{\parallel}$, which makes $\sigma_{\perp}$ more apt for actual stress measurements on single-domain surfaces, e.g., by the

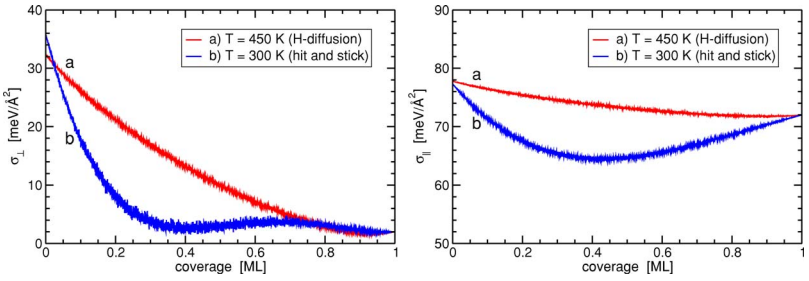

FIG. 6. (Color online) Simulated coverage dependence of the stresses $\sigma_{\perp}$ and $\sigma_{\parallel}$. The blue curve corresponds to hit and stick H adsorption without H diffusion (i.e., the hydrogen atoms are distributed randomly over the silicon surface), whereas the red curve represents results for a thermodynamically equilibrated surface (assuming that the hydrogen atoms can diffuse on the surface).

method of surface stress induced optical deflection (SSIOD).[42–44]

By applying a simple averaging scheme, the stress of macroscopic partially H-covered Si(001) surfaces has been estimated. We find a more tensile stress in the case of the equilibrated structure because of the thermal quenching of high-surface-energy configurations. We speculate that this variation of surface stress at fixed hydrogen coverage due to the disappearance of high-surface-energy configurations could be used to monitor hydrogen diffusion on Si(001) surfaces prepared by adsorption of atomic hydrogen at temperatures close to the onset of diffusion. This would complement diffusion measurements by second harmonic generation (SHG) methods.[46]

Finally, our calculations emphasize the important role that the Jahn-Teller-like coupling between dangling bonds plays for the dimer buckling. On partially H-covered Si(001) surfaces, this coupling occurs also between dangling-bond orbitals located on neighboring dimers; it is not restricted to dangling-bond orbitals on one and the same dimer. Moreover, the sensitive dependence of stress, in particular $\sigma_\perp$, on the particular adsorption geometry is pointed out.

TABLE V. Comparison of $\sigma_\perp$, $\sigma_\parallel$ and $\Delta\sigma$ between the total energy method using the FHI96MD code and the analytical stress tensor method using the ABINIT code.

	$\sigma_\parallel$	$\sigma_\perp$ FHI96MD	$\Delta\sigma$	$\sigma_\parallel$	$\sigma_\perp$ ABINIT	$\Delta\sigma$
Coverage			(meV/Å^2)			
$\Theta=0$, $p(2\times2)$	77	38	39	79	39	40
$\Theta=1$, monohydride	72	2	70	76	6	70
$\Theta=1/2$, monohydride	70	−4	78	78	2	76
$\Theta=1/2$, *cis*	60	29	31	61	30	32
$\Theta=1/2$, *trans*	58	22	39	67	27	40
$\Theta=1/4$, config. I	60	1	57	66	9	58
$\Theta=1/4$, config. II	59	−50	107	62	−43	106
$\Theta=3/4$, spin unpol.	66	−2	73	70	−2	71

ACKNOWLEDGMENTS

We are grateful to M. Horn von Hoegen for his support of this work, which started in his research group at the University of Essen, and to him and P. Kury for many enlightening discussions.

APPENDIX: COMPARISON TO ANALYTICAL STRESS TENSOR

Although in our work reported in this paper the stress tensor components have been calculated directly from total-energy differences as a function of strain, the stresses can also be calculated using an analytical stress tensor.[29] In that case, only a single density-functional calculation at the equilibrium constant has to be carried out. For this approach it is important to carefully determine the theoretical equilibrium lattice constant, because otherwise large contributions from the bulk stress would add to the surface stress and degrade the accuracy of the result. (In principle, this problem could again be circumvented by doing calculations for slabs of different thickness and eliminating the bulk stress, but this more elaborate approach is beyond the purpose of the simple test calculations reported here.)

To compare both methods we have carried out additional calculations using the ABINIT code,[28] which makes use of the analytical stress tensor. We use 12 atomic layers to keep contributions from the bulk stress as small as possible and the interaction between the two surfaces at each side of the slab as small as necessary. The other parameters, cutoff energy, number of **k**-points, thickness of vacuum region and pseudopotential, are the same as in the total energy calculations with FHI96MD described in Sec. II. There is good agreement between the two methods within the error bars (see Table V). A small but systematic difference in the range of some meV/Å^2 toward tensile stress can be found in $\sigma_\perp$ and $\sigma_\parallel$, this being a hint that in the calculation the lattice constant may have been chosen slightly too large. In case of the stress anisotropy $\Delta\sigma$ the contributions from bulk stress cancel and the differences between the two approaches are even smaller.

*Electronic address: pehlke@theo-physik.uni-kiel.de

[1] H. Ibach, Surf. Sci. Rep. **29**, 193 (1997).
[2] P. Müller and A. Saúl, Surf. Sci. Rep. **54**, 157 (2004).
[3] F. Bechstedt, *Principles of Surface Physics*, Series: Advanced Texts in Physics (Springer-Verlag, Berlin, 2003).
[4] O. H. Nielsen and R. M. Martin, Phys. Rev. Lett. **50**, 697 (1983).
[5] W. Haiss, Rep. Prog. Phys. **64**, 591 (2001).
[6] R. D. Meade and D. Vanderbilt, Phys. Rev. Lett. **63**, 1404 (1989).
[7] S. B. Healy, C. Filippi, P. Kratzer, E. Penev, and M. Scheffler, Phys. Rev. Lett. **87**, 016105 (2001).
[8] K. W. Kolasinski, W. Nessler, A. de Meijere, and E. Hasselbrink, Phys. Rev. Lett. **72**, 1356 (1994).
[9] M. Dürr, M. B. Raschke, E. Pehlke, and U. Höfer, Phys. Rev. Lett. **86**, 123 (2001).
[10] W. Brenig, H. J. Kreuzer, and S. H. Payne, Phys. Rev. B **67**, 205419 (2003).
[11] F. Liu and M. G. Lagally, Phys. Rev. Lett. **76**, 3156 (1996).
[12] R. D. Meade and D. Vanderbilt, in *The Physics of Semiconductors*, edited by E. M. Anastassakis and J. D. Joannopoulos (World Scientific, Singapore, 1990), p. 123.
[13] A. Garcia and J. E. Northrup, Phys. Rev. B **48**, 17350 (1993).
[14] M. C. Payne, N. Roberts, R. J. Needs, M. Needels, and J. D.

Joannopoulos, Surf. Sci. **211/212**, 1 (1989).
[15] O. L. Alerhand, D. Vanderbilt, R. D. Meade, and J. D. Joannopoulos, Phys. Rev. Lett. **61**, 1973 (1988).
[16] J. Dąbrowski, E. Pehlke, and M. Scheffler, Phys. Rev. B **49**, 4790 (1994).
[17] A. Biedermann, E. Knoesel, Z. Hu, and T. F. Heinz, Phys. Rev. Lett. **83**, 1810 (1999).
[18] E. Pehlke, Phys. Rev. B **62**, 12932 (2000).
[19] U. Höfer, L. Li, and T. F. Heinz, Phys. Rev. B **45**, R9485 (1992).
[20] M. Bockstedte, A. Kley, J. Neugebauer, and M. Scheffler, Comput. Phys. Commun. **107**, 187 (1997).
[21] J. P. Perdew, K. Burke, and M. Ernzerhof, Phys. Rev. Lett. **77**, 3865 (1996).
[22] M. Fuchs and M. Scheffler, Comput. Phys. Commun. **116**, 1 (1999).
[23] H. J. Monkhorst and J. D. Pack, Phys. Rev. B **13**, 5188 (1976).
[24] G.-M. Rignanese, Ph. Ghosez, J.-C. Charlier, J.-P. Michenaud, and X. Gonze, Phys. Rev. B **52**, 8160 (1995).
[25] M. Fuchs, M. Bockstedte, E. Pehlke, and M. Scheffler, Phys. Rev. B **57**, 2134 (1998).
[26] By this choice of ε_{zz} the elastic energy of the strained bulk is minimized. Because the stress perpendicular to the surface vanishes, $\sigma_{zz}=0$, the calculation of the surface stress is not affected.
[27] O. Madelung, *Semiconductors: Data Handbook* (Springer, Berlin, 2004).
[28] X. Gonze, J.-M. Beuken, R. Caracas, F. Detraux, M. Fuchs, G.-M. Rignanese, L. Sindic, M. Verstraete, G. Zerah, F. Jollet, M. Torrent, A. Roy, M. Mikami, Ph. Ghosez, J.-Y. Raty, and D. C. Allan, Comput. Mater. Sci. **25**, 478 (2002).
[29] O. H. Nielsen and R. M. Martin, Phys. Rev. B **32**, 3780 (1985); **32**, 3792 (1985); A. Dal Corso and R. Resta, *ibid.* **50**, 4327 (1994).
[30] G. P. Francis and M. C. Payne, J. Phys.: Condens. Matter **2**, 4395 (1990).
[31] A. Ramstad, G. Brocks, and P. J. Kelly, Phys. Rev. B **51**, 14504 (1995).
[32] J. Dąbrowski, E. Pehlke, and M. Scheffler, J. Vac. Sci. Technol. B **12**, 2675 (1994).
[33] C. Filippi, S. B. Healy, P. Kratzer, E. Pehlke, and M. Scheffler, Phys. Rev. Lett. **89**, 166102 (2002).
[34] P. Krüger and J. Pollmann, Phys. Rev. Lett. **74**, 1155 (1995).
[35] M. B. Webb, F. K. Men, B. S. Swartzentruber, R. Kariotis, and M. G. Lagally, Surf. Sci. **242**, 23 (1991).
[36] M. C. Flowers, N. B. H. Jonathan, A. Morris, and S. Wright, J. Chem. Phys. **108**, 3342 (1998).
[37] E. Pehlke and P. Kratzer, Phys. Rev. B **59**, 2790 (1999).
[38] J. J. Boland, Phys. Rev. Lett. **67**, 1539 (1991).
[39] Note, however, that these energies correspond to periodically repeated *cis*- and *trans*-configurations and thus do not necessarily reflect the energy of an isolated adsorbate group.
[40] M. Bockstedte (private communication), see also Ref. 20.
[41] P. Kratzer, J. Chem. Phys. **106**, 6752 (1997).
[42] A. J. Schell-Sorokin and R. M. Tromp, Phys. Rev. Lett. **64**, 1039 (1990).
[43] P. Zahl, P. Kury, and M. Horn-von Hoegen, Appl. Phys. A: Mater. Sci. Process. **69**, 481 (1999).
[44] P. Kury, T. Grabosch, and M. Horn-von Hoegen, Rev. Sci. Instrum. **76**, 023903 (2005).
[45] N. Metropolis, A. W. Rosenbluth, M. N. Rosenbluth, A. H. Zeller, and E. Zeller, J. Chem. Phys. **21**, 1087 (1953).
[46] G. A. Reider, U. Höfer, and T. F. Heinz, Phys. Rev. Lett. **66**, 1994 (1991).
[47] These results have been calculated with ABINIT.